J Mater Sci (2012) 47:1026–1032
DOI 10.1007/s10853-011-5890-0

A facile synthesis of graphene–metal (Pb, Zn, Cd, Mn) sulfide composites

Xiaoqi Fu · Tingshun Jiang · Qian Zhao · Hengbo Yin

Received: 11 July 2011 / Accepted: 19 August 2011 / Published online: 3 September 2011

Abstract We propose a general approach for the preparation of graphene-metal sulfide quantum dots (QDs) composites by π–π stacking of pyridine-capped metal sulfide QDs and chemically converted graphene (CCG) in aqueous solution. CCG sheets disperse stably in water without the assistance of dispersing agents, only by electrostatic repulsion. The aromatic structures of pyridine capped on metal sulfide QDs make these QDs dispersible in ethanol or water, and further introduce a π–π stacking interaction between CCG and QDs, and extend the conjugated structure of CCG. The structural details, formation mechanism, and textural properties of the resultant graphene-metal sulfide QDs composites are characterized by X-ray diffraction, UV–vis absorption, electron microscopy, and Raman scattering studies. The CCG–metal sulfide composites disperse stably in aqueous solution, allowing them to be potentially used in biological tissues and easy-to-form filtered films for further research and application.

Introduction

Graphene, a monolayer of sp^2-bonded carbon atoms packed into a honeycomb crystal plane, has triggered considerable research interests in recent years, owing to its extraordinary mechanical [1], electronic properties [2], and potential application in sensors [3], integrated circuits [4], catalysis [5, 6], ultra capacitors [7], and new graphene devices [8]. However, without any unstable bonds on its surface, perfect graphene is highly chemically stable, resulting in inert surface, weak interaction with other mediums and insolubility in water and common organic solvents, which becomes an obstacle in its further research and application.

Graphite oxide (GO) obtained by oxidation of graphite exhibits good solubility and intercalation properties and allows interlayer accommodation of several materials for GO composites [9–11], owing to the presence of the hydrophilic polar groups in the interlayer. However, the intercalated oxygen functional groups break the graphene π-conjugated structure, making the conductivity and other properties of graphene significantly decreased [12, 13].

As Li et al. [14] recently demonstrated that chemically converted graphene (CCG) sheets obtained from GO can readily form stable aqueous colloids without the assistance of dispersing agents, only by electrostatic repulsion. The dissolution of graphene sheets in water as well as the carboxylic groups remains intact on the edge of graphene sheets after hydrazine reduction enables the use of solution-phase chemistry to further modify graphene sheets for achieving new functionalities and devices [14]. Aqueous soluble CCG allows for π-stacking of various aromatic molecules, such as polystyrene [15], pyrenebutyrate [16], poly(3,4-ethylenedioxythiophene) [17], and so on. Geng et al. [18] have obtained graphene–CdSe π–π stacking composites for transparent optoelectronic films. Here, we report on the preparation of CCG–metal sulfide quantum dots (CCG-MS) π-stacking composites. The sulfide QDs (PbS, ZnS, CdS and MnS) capped with pyridine were dispersible in ethanol. The CCG–MS composites were synthesized by π–π stacking of aromatic structures between CCG and pyridine-capped MS QDs.

X. Fu (✉) · T. Jiang · Q. Zhao · H. Yin
School of Chemistry and Chemical Engineering, Jiangsu University, Zhenjiang 212013, People's Republic of China
e-mail: xfu@ujs.edu.cn

X. Fu
School of Material Science and Engineering, Jiangsu University, Zhenjiang 212013, People's Republic of China

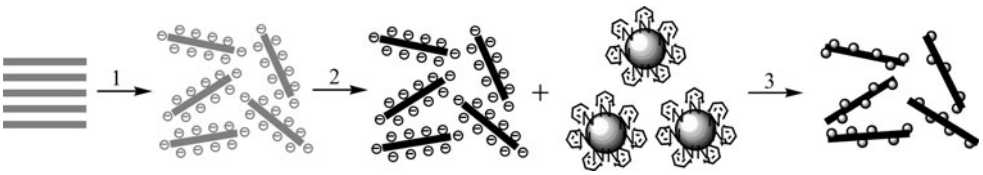

Fig. 1 Schematic of the fabrication process for CCG–MS composites

MS QDs are of great interest because of their quantum confinement effects and size-dependent properties and have been widely used in electronics, magnetics, optics, biology, and chemistry [19, 20]. Nethravathi et al. [21] have prepared graphene–CdS and graphene–ZnS composites by mixing GO with $Cd(NO_3)_2$ and $Zn(NO_3)_2$ solutions, respectively. Cao et al. [22] have successfully synthesized graphene–CdS complex using dimethylsulfoxide as solvent and sulfur as source. However, these in situ routes may lead to many defects and residual hydroxyl and epoxide groups on the graphene layers [10, 23], which destroy the graphene π-conjugated structure and significantly decrease the outstanding properties of graphene. Hence, aqueous soluble CCG solution and pyridine-capped MS QDs in ethanol were used for preparing CCG-MS π-stacking composites. In addition, Raman scattering was used for investigating the conjugated structure details.

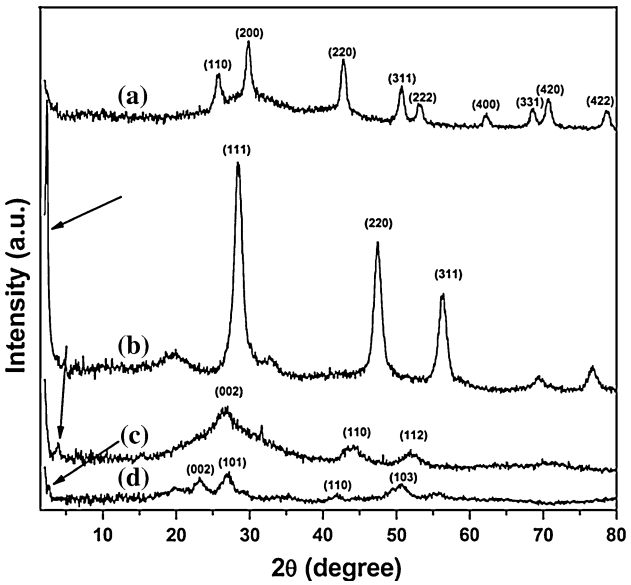

Fig. 2 XRD patterns of the CCG–MS composites: (*a*) CCG–PbS, (*b*) CCG–ZnS, (*c*) CCG–CdS, and (*d*) CCG–MnS

Experimental section

Syntheses of MS quantum dots

The MS QDs were prepared according to the following procedure [24–26]

$PbCl_2$ (1 mmol) and oleylamine (OLA, 5 mL) were mixed together under vacuum at 100 °C for 1 h to form a special Pb–OLA complex. Then, the mixture was kept under nitrogen at 100 °C for another 5 min. A solution of 0.67 mmol sulfur in 2.5 mL OLA was quickly injected into the Pb–OLA complex solution. The resulting mixture was rapidly heated to 210 °C and held for 1 h and then cooled to room temperature.

$ZnCl_2$ (2 mmol), poly(ethylene glycol) (2.5 g, MW 10 000), and OLA (5 mL) were mixed together under vacuum at 170 °C for 1 h to form a Zn–OLA complex. Then, the mixture was kept under nitrogen at 170 °C for another 5 min. A solution of 6 mmol sulfur in 5 mL OLA was quickly injected into the Zn–OLA complex solution. The resulting mixture was rapidly heated to 290 °C and held for 1 h.

$CdCl_2$ (1.5 mmol) and oleylamine (OLA, 5 mL) were mixed together under vacuum at 160 °C for 1 h to form a special Cd–OLA complex. Then, the mixture was kept under nitrogen at 160 °C for another 5 min. A solution of

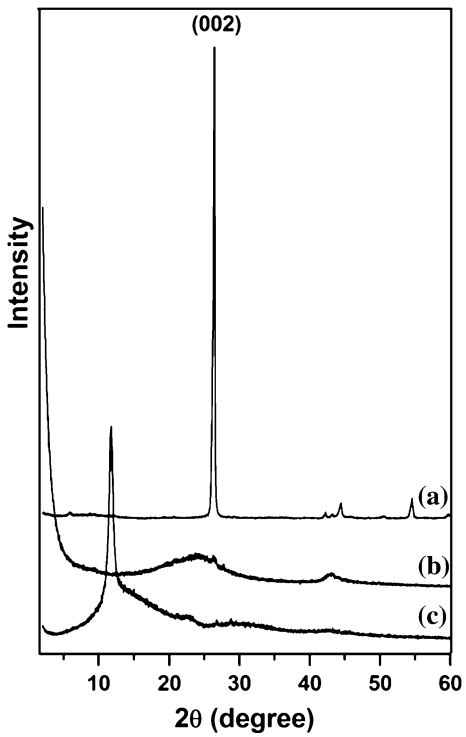

Fig. 3 XRD patterns of *a* raw graphite, *b* CCG, and *c* GO

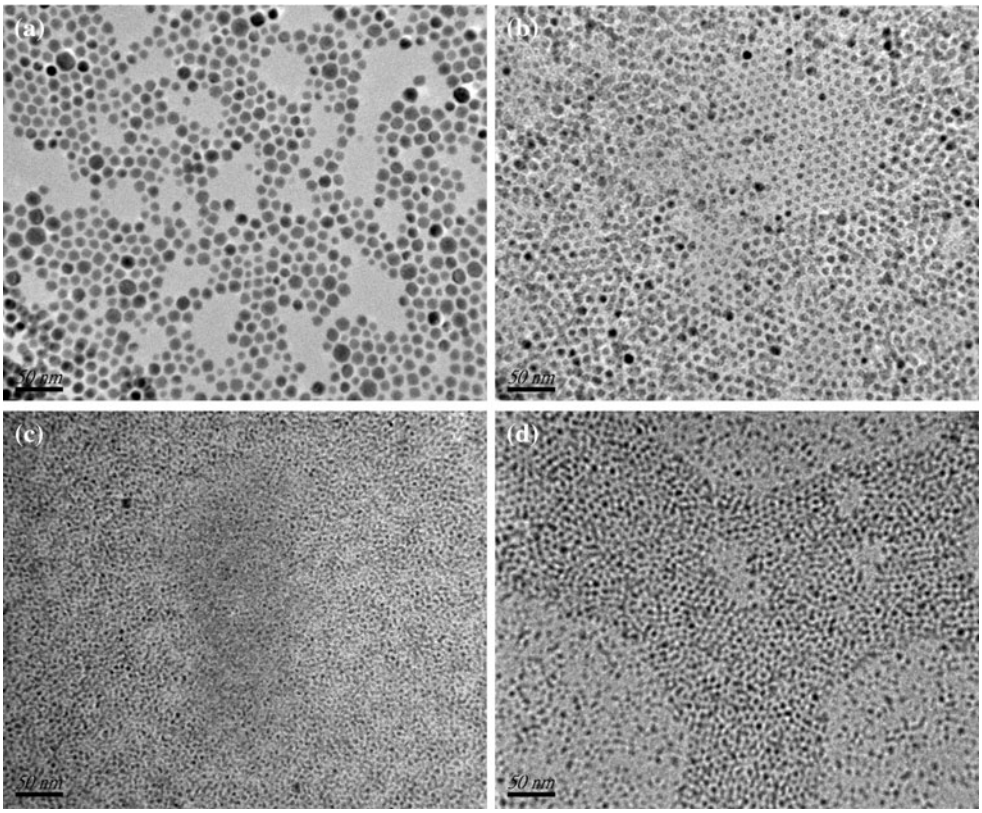

Fig. 4 TEM images of **a** PbS, **b** ZnS, **c** CdS, and **d** MnS nanoparticles

0.75 mmol sulfur in 2.5 mL OLA was quickly injected into the Cd–OLA complex solution. The resulting mixture was aged at 160 °C for 6 h.

$MnCl_2$ (3 mmol) and oleylamine (OLA, 5 mL) were mixed together under vacuum at 120 °C for 1 h to form a special Mn–OLA complex. Then, the mixture was kept under nitrogen at 120 °C for another 5 min. A solution of 1 mmol sulfur in 2.5 mL OLA was quickly injected into the Mn–OLA complex solution. The resulting mixture was rapidly heated to 290 °C and held for 6 h.

MS QDs were separated by adding cold ethanol followed by centrifugation.

Syntheses of pyridine-capped MS quantum dots

The resulting MS QDs were dispersed well in toluene (15 mL). The pyridine-capped MS QDs were prepared by Geng's method [18]. 20 mL anhydrous pyridine was added into the resulting OLA-capped MS QDs toluene dispersion (5 mL), and refluxed at 118 °C under nitrogen for 24 h. The solution was centrifuged after adding hexane. The ligand exchange process was repeated for three times. The obtained pyridine-capped MS QDs were dispersed in ethanol (20 mL).

Synthesis of chemically converted graphene (CCG)

GO was prepared from purified natural graphite (230 mesh, Qingdao Zhongtian Company) according to the method reported by Hummers and Offeman [27]. CCG was synthesized by the Li's method [14]. The obtained GO product was washed with ultrapure water until attaining a neutral pH and then dispersed in water to form a $\sim$13.4 mg/mL GO dispersion. All the water used in the preparation was distilled through Molecular water purification system with a resistivity of 18.2 MΩ. A 1.5 mL of the above GO dispersion was dissolved in water via ultrasonic for 45 min, to form a 1 mg/mL exfoliated GO dispersion. The homogeneous dispersion was mixed with 23.25 μL of hydrazine solution (85%) and 440 μL of ammonia solution (25%) in a 50 mL glass vial under vigorously stirred for 10 min, and then heated to 95 °C for 1 h. Clear CCG solution was obtained after the mixture was centrifuged at 6000 rpm. for 10 min to remove the large graphene particles.

Syntheses of CCG–MS composites

The CCG–MS composites were synthesized by mixing 5 mL of pyridine-capped MS QDs in ethanol solution with

20 mL CCG solution under magnetic stirring at 60 °C for 12 h (Fig. 1).

Sample characterization

X-Ray diffraction (XRD) patterns of MS QDs and CCG–MS composites were recorded on a Bruker D8 Advanced X-ray diffractometer using Cu-Kα radiation ($\lambda = 0.1542$ nm). The morphologies of samples were observed by transmission electron microscope (TEM, JEM-2100). The electronic absorption spectra were recorded on a Shimadzu UV-2450 UV–vis spectrophotometer with standard 1-cm optical path quartz cells. Raman spectra were recorded on a Renishaw Invia Raman Microscope using a 514.5-nm argon ion laser.

Results and discussion

We describe our graphene composite samples as graphene–metal sulfide π-stacking composites, CCG–PbS, CCG–ZnS, CCG–CdS and CCG–MnS, prepared by π–π stacking of CCG and pyridine-capped metal sulfide QDs. X-ray powder diffraction (XRD) patterns of the resulting CCG–MS composites are illustrated in Fig. 2. After CCG had been dried from aqueous colloids, the graphene sheets tend to form aggregations and even restack to form graphite. It is evidenced by the appearance of diffraction peak of bulk CCG at around $2\theta \approx 25°$ (Fig. 3) with, the interlayer space being about 0.35 nm, similar to (002) reflection of raw graphite. This broadened peak disappears in the XRD pattern of CCG–PbS, CCG–ZnS, CCG–CdS and CCG–MnS; instead, a new diffraction peak of CCG–MS appears at low angle, CCG–ZnS at $2\theta = 2.38°$ (3.8 nm), CCG–CdS at $2\theta = 3.9°$ (2.3 nm) and CCG–MnS at $2\theta = 2.6°$ (3.3 nm), and the other peaks are all ascribed to the characteristic Bragg reflections of PbS [28], ZnS [25], CdS [29], and MnS [30], respectively. It is indicated that the attachments of these MS QDs onto CCG graphene sheets prevent the restack of graphene sheets, and they form a new class of CCG-based composites. It needs to be noted that the intensities of these low-angle diffraction peaks are very week, except that of CCG–ZnS. Recent studies [10, 31] have shown that, if the regular stacks of GO or graphene are destroyed, for example, by exfoliation, their diffraction peaks become weak or even disappear. This may be the reason that we did not see the low-angle diffraction peak of CCG–PbS in Fig. 2a.

Figure 4 shows the TEM images of MS QDs, revealing uniform 10-, 5.5-, 4-,and 5-nm-sized nanocrystals for PbS, ZnS, CdS and MnS, respectively. After removing the capping ligands (OLA) of MS QDs, the actual sizes of MS QDs have a good agreement with the corresponding XRD results at low-angle diffraction. These nanocrystals shape

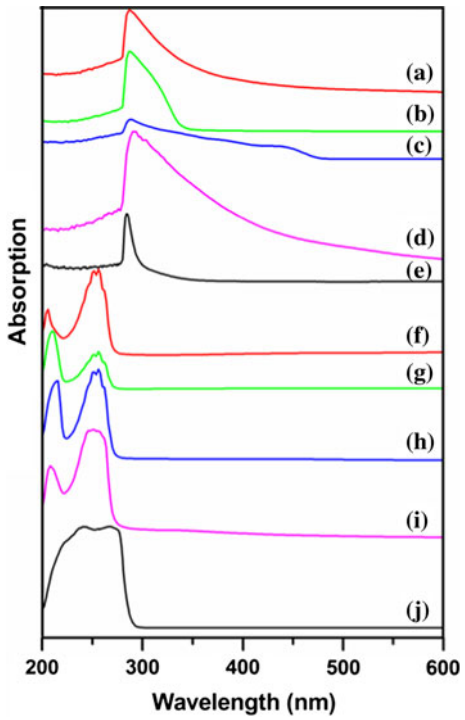

Fig. 5 Absorption spectra of (*a*) PbS, (*b*) ZnS, (*c*) CdS, (*d*) MnS, and (*e*) OLA dispersed in toluene. The absorption peaks at ~287 nm are ascribed to C=C π–π electron transition of OLA. The shoulder peaks in (*b*) and (*c*) are assigned to ZnS and CdS, respectively; Absorption spectra of (*f*) PbS, (*g*) ZnS, (*h*) CdS, (*i*) MnS, and (*j*) pyridine dispersed in ethanol after refluxing with pyridine. The double peaks are assigned to pyridine. All spectra are obtained from the diluted solution

are nearly spherical and highly monodispersed. They are well dispersible in toluene or hexane. It needs to be noted that the particles size and shape of these MS nanocrystals can be controlled by changing the relative amounts of metal precursor and sulfur, injection temperature, and growth temperature. These highly monodispersed MS QDs can be applied in many areas, such as PbS with a band gap energy of 0.41 eV being used in biological labeling and diagnostics, light-emitting diodes, electroluminescent devices, photovoltaic devices, lasers, and single-electron transistors [32, 33]. After changing the capping agent of MS QDs from OLA to pyridine, the pyridine-capped MS QDs are dispersible in ethanol or water. We compare the absorption spectra of pyridine-capped MS QDs in ethanol and OLA-capped MS QDs in toluene (Fig. 5). The spectra are quite different after the capping agents were changed; the absorption peaks at ~287 nm corresponding to OLA disappear; and the double absorption peaks ranging from 200 to 280 nm corresponding to pyridine appear, indicating that the ligands of MS QDs are almost completely exchanged with pyridine by refluxing in pyridine. In addition, the two peaks overlapping side by side corresponding to pyridine split into two separate peaks after ligand changing: the first

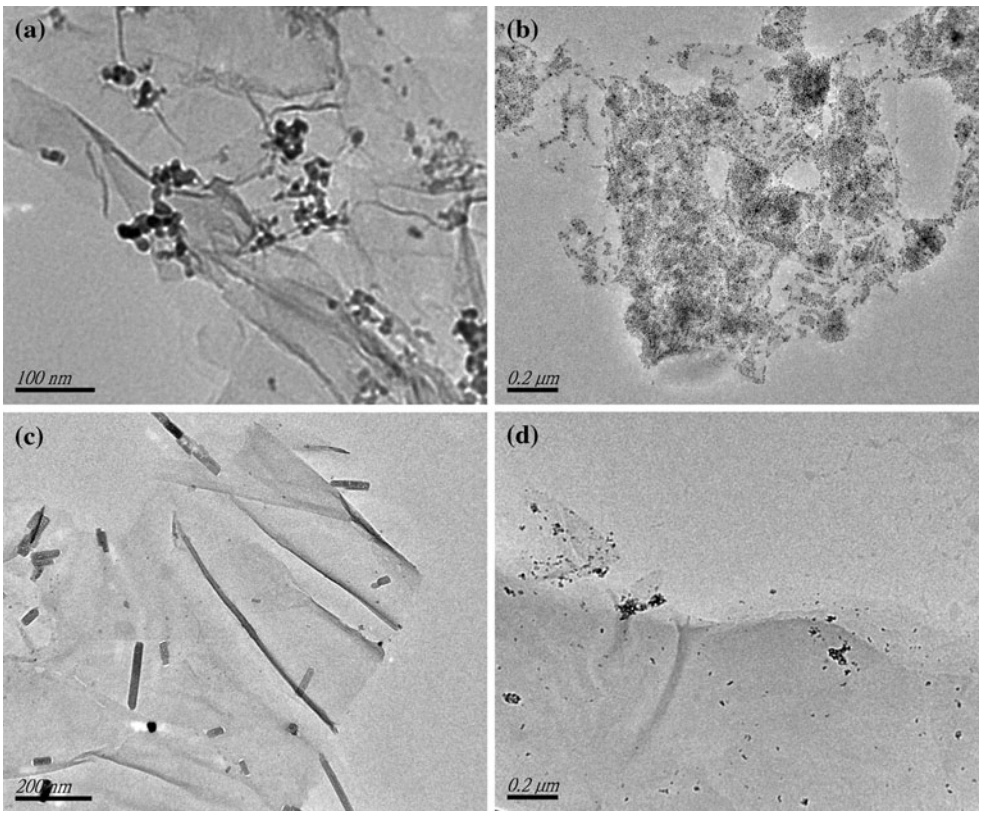

Fig. 6 TEM images of the resulting **a** CCG–PbS, **b** CCG–ZnS, **c** CCG–CdS, and **d** CCG–MnS composites

one at 255 nm is assigned to C=C π–π electron transition. The second one at around 210 nm assigned to C=N π–π electron transition shows some shift for PbS (206 nm), ZnS (210 nm), CdS (215 nm) and MnS (208 nm), because of the influence of pyridine absorbed on MS QDs through N atoms.

In general, MS QDs are synthesized in organic medium, and these contain a layer of outside-capping ligand, which makes them insoluble in aqueous solution. After changing the capping agent to pyridine, MS QDs become water soluble. Considering that the unique optoelectronic properties of MS QDs and CCG possess large surface areas act as carrier, CCG–MS composites were expected to have large potential applications in biological tissues, such as biosensing and bioimaging. Attachments of MS QDs to CCG can be verified by the morphologic analyses of electron microscope images. Figure 6 shows the TEM images of CCG–PbS, CCG–ZnS, CCG–CdS, and CCG–MnS composites. It is clearly seen that most MS QDs distribute randomly on the almost transparent carbon sheets, and a few particles were scattered out of the supports. It seems that the QDs particles locate firmly on CCG sheets by noncovalent bond. Although there are some large particles on CCG sheets, most QDs particles distribute randomly on the sheets without obvious size and shape change, and obvious aggregations.

The π–π stacking structure of these composites can also be supported by the analyses of Raman scattering. Raman spectroscopy is a powerful technique to provide detailed information as to molecular structures and has proved to be a useful tool for the characterization of carbon products, especially considering the fact that conjugated and double carbon–carbon bonds lead to high Raman intensities [34–36]. The most prominent features for graphene materials in Raman spectra are the G band (around 1582 cm^{-1} using laser excitation at 2.41 eV) which is associated with the E_{2g} phonon of sp^2 atoms, and the D band (around 1350 cm^{-1}) which is the result of the breathing mode of k-point phonons of A_{1g} [10]. After chemical reduction of GO by hydrazine, the oxygen functional groups in GO sheets can be removed, and the conjugated graphene network will be re-established. However, the size of the reestablished graphene network was smaller than the original ones, leaving topological defects and vacancies, which makes the intensity ratio of D/G to increase [34, 37]. It is interesting to note that the D/G ratios of CCG–MS composites were decreased after π–π stacking of pyridine-capped MS QDs on CCG planes (Fig. 7). This is quite

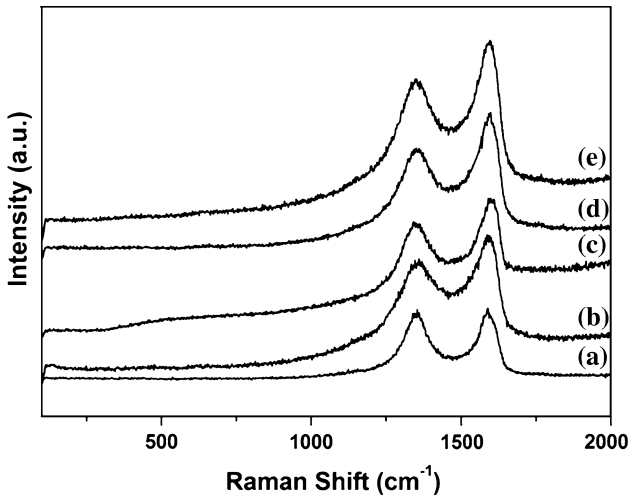

Fig. 7 Raman spectra of (*a*) bulk CCG, (*b*) CCG–PbS, (*c*) CCG–ZnS, (*d*) CCG–CdS, and (*e*) CCG–MnS composites

different from the previous graphene–metal composites grown in situ method, in which the D/G ratios increase even more than 1 [10, 38]. We consider that the aromatic structures of pyridine capped on MS QDs extend the conjugated structure of CCG, and then make the intensity ratio of D/G to decrease. This makes sense with respect to the formation of more extended networks of conjugated sp^2 carbons, toward a more locally ordered graphene lattice. In addition, it should be noted that the differences in the D/G ratios can be found in the Raman spectra of CCG–MS composites (Fig. 7b, c, d, e), because of the nanoparticles size and activity are different from each other.

The CCG–MS filtered films, shown in Fig. 8, were prepared by vacuum filtration of the dispersions of CCG–MS through a mixed cellulose–ester membrane with a pore size of 0.45 μm. Considering the unique optoelectronic properties of MS QDs and that CCG possess large specific surface areas, we expect that the CCG–MS filtered films would present some special features, such as photosensitivity, photoconductivity and catalysis. It should be mentioned here that the resultant CCG–MS filtered films are frangible, comparing with CCG filtered film.

Conclusion

In summary, we have demonstrated that CCG-MS composites can be fabricated by π–π stacking of CCG and MS QDs. In our system, MS QDs are dispersible in ethanol or water after the capping agent changed from OLA to pyridine, and then noncovalently coupled to CCG sheets in aqueous solutions. The aqueous dispersibility of CCG-MS composites enables such composites to become particularly useful in certain technological applications, such as biosensing and bioimaging, and forming filtered films for unique optoelectronic properties.

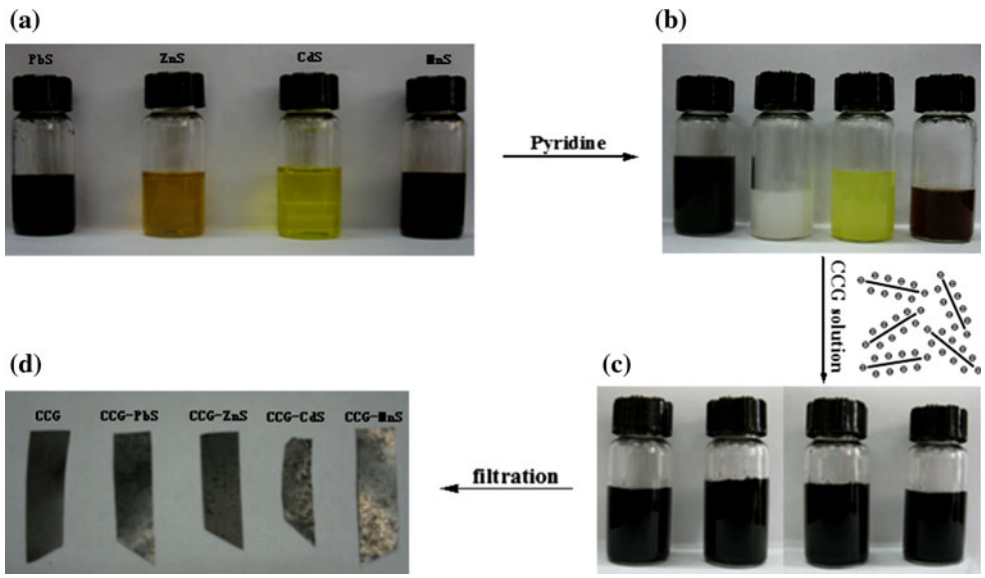

Fig. 8 The fabrication process of CCG–MS filtered films. **a** The photograph shows that PbS, ZnS, CdS, and MnS are dispersible in toluene, even after several months. **b** PbS, ZnS, CdS, and MnS are dispersible in ethanol after ligands are changed from OLA to pyridine. It should be noted that the ZnS ethanol dispersion was not stable and left some precipitate at bottom of bottle after several hours. However, on heating up to ~65 °C, it would become a clear yellowy solution. **c** The photograph shows that the resulting CCG–MS composites are dispersible in aqueous solution, although some large particles float above the water. It can be removed by centrifugation. **d** The photograph of resulting CCG-MS filtered films

Acknowledgement This study was supported by the Natural Science Foundation of Jiangsu Higher Education Institutions of China (09KJD150002), Zhenjiang Science and Technology Bureau (GJ2006006) and Jiangsu University High-grade Specialty Person Scientific Research Foundation (10JDG114).

References

1. Lee C, Wei X, Kysar JW, Hone J (2008) Science 321:385
2. Avouris P, Chen Z, Perebeinos V (2007) Nat Nanotechnol 2:605
3. Schedin F, Geim AK, Morozov SV, Hill EW, Blake P, Katsnelson MI, Novoselov KS (2007) Nat Mater 6:652
4. Chen J, Ishigami M, Jang C, Hines DR, Fuhrer MS, Williams ED (2007) Adv Mater 19:3623
5. Jasuja K, Berry V (2009) ACS Nano 3:2358
6. Si YC, Samulski ET (2008) Chem Mater 20:6792
7. Stoller MD, Park S, Zhu Y, An J, Ruoff RS (2008) Nano Lett 8:3498
8. Echtermeyer TJ, Lemme MC, Baus M, Szafranek BN, Geim AK, Kurz H (2008) IEEE Electron Device Lett 29:952
9. Zhang Y, Pan C (2011) J Mater Sci 46:2622. doi:10.1007/s10853-010-5116-x
10. Fu X, Bei F, Wang X, O'Brien S, Lombardi JR (2010) Nanoscale 2:1461
11. Chang L, Wu S, Chen S, Li X (2011) J Mater Sci 46:2024. doi:10.1007/s10853-010-5033-z
12. Gómez-Navarro C, Weitz RT, Bittner AM, Scolari M, Mews A, Burghard M, Kern K (2007) Nano Lett 7:3499
13. Cote LJ, Cruz-Silva R, Huang J (2009) J Am Chem Soc 131:11027
14. Li D, Muller MB, GiljE S, Kaner RB, Wallace GG (2008) Nat Nanotechnol 3:101
15. Li XL, Wang XR, Zhang L, Lee SW, Dai HJ (2008) Science 319:1229
16. Xu YX, Bai H, Lu GW, Li C, Shi GQ (2008) J Am Chem Soc 130:5856
17. Hong WJ, Xu YX, Lu GW, Li C, Shi GQ (2008) Electrochem Commun 10:1555
18. Geng X, Niu L, Xing Z, Song R, Liu G, Sun M, Cheng G, Zhong H, Liu Z, Zhang Z, Sun L, Xu H, Lu L, Liu L (2010) Adv Mater 22:638
19. Cademartiri L, Montanari E, Calestani G, Migliori A, Guagliardi A, Ozin GA (2006) J Am Chem Soc 128:10337
20. Wang Q, Seo DK (2009) J Mater Sci 44:816. doi:10.1007/s10853-008-3138-4
21. Nethravathi C, Viswanath B, Shivakumara C, Mahadevaiah N, Rajamathi M (2008) Carbon 46:1773
22. Cao AN, Liu Z, Chu SS, Wu MH, Ye ZM, Cai ZW, Chang YL, Wang SF, Gong QH, Liu YF (2009) Adv Mater 21:103
23. Soldano C, Mahmood A, Dujardin E (2010) Carbon 48:2127
24. Joo J, Na HB, Yu T, Yu JH, Kim YW, Wu F, Zhang JZ, Hyeon T (2003) J Am Chem Soc 125:11100
25. Quan Z, Wang Z, Yang P, Lin J, Fang J (2007) Inorg Chem 46:1354
26. Fu X, Pan Y, Wang X, Lombardi JR (2011) J Chem Phys 134:024707
27. Hummers WS, Offeman RE (1958) J Am Chem Soc 80:1339
28. Cademartiri L, Bertolotti J, Sapienza R, Wiersma DS, von Freymann G, Ozin GA (2006) J Phys Chem B 110:671
29. Pawar MJ, Chaure SS (2009) Chalcogenide Lett 6:689
30. Fan DB, Wang H, Zhang YC, Cheng J, Yan H (2004) Surf Rev Lett 11:27
31. Cai DY, Song M (2007) J Mater Chem 17:3678
32. Hyun BR, Zhong YW, Bartnik AC, Sun L, Abruna HD, Wise FW, Goodreau JD, Matthews JR, Leslie TM, Borrelli NF (2008) ACS Nano 2:2206
33. Gocalinska A, Saba M, Quochi F, Marceddu M, Szendrei K, Gao J, Loi MA, Yarema M, Seyrkammer R, Heiss W, Mura A, Bongiovanni G (2010) J Phys Chem Lett 1:1149
34. Kudin KN, Ozbas B, Schniepp HC, Prud'homme RK, Aksay IA, Car R (2008) Nano Lett 8:36
35. Rourke JP, Pandey PA, Moore JJ, Bates M, Kinloch IA, Young RJ, Wilson NR (2011) Angew Chem Int Ed 50:3173
36. Wilson NR, Pandey PA, Beanland R, Young RJ, Kinloch IA, Gong L, Liu Z, Suenaga K, Rourke JP, York SJ, Sloan J (2009) ACS Nano 3:2547
37. Wang G, Yang J, Park J, Gou X, Wang B, Liu H, Yao J (2008) J Phys Chem C 112:8192
38. Xu C, Wang X, Zhu J (2008) J Phys Chem C 112:19841